



Swansea University
Prifysgol Abertawe



Cronfa - Swansea University Open Access Repository

This is an author produced version of a paper published in:
IEEE Transactions on Industrial Electronics

Cronfa URL for this paper:

<http://cronfa.swan.ac.uk/Record/cronfa39381>

Paper:

Li, Z., Huang, B., Ye, Z., Deng, M. & Yang, C. (2018). Physical Human-Robot Interaction of a Robotic Exoskeleton By Admittance Control. *IEEE Transactions on Industrial Electronics*, 1-1.

<http://dx.doi.org/10.1109/TIE.2018.2821649>

This item is brought to you by Swansea University. Any person downloading material is agreeing to abide by the terms of the repository licence. Copies of full text items may be used or reproduced in any format or medium, without prior permission for personal research or study, educational or non-commercial purposes only. The copyright for any work remains with the original author unless otherwise specified. The full-text must not be sold in any format or medium without the formal permission of the copyright holder.

Permission for multiple reproductions should be obtained from the original author.

Authors are personally responsible for adhering to copyright and publisher restrictions when uploading content to the repository.

<http://www.swansea.ac.uk/library/researchsupport/ris-support/>

Admittance Control of a Robotic Exoskeleton for Physical Human Robot Interaction

Bo Huang, Zhijun Li and Chenguang Yang

Abstract—In this paper, an admittance control scheme is proposed for physical human-robot interaction with human subject's intention motion as well as dynamic uncertainties of the robotic exoskeleton. Human subject's intention motion is represented by the reference trajectory when the exoskeleton manipulator is complying with the external interaction force. Online estimation of the stiffness is employed to deal with the variable impedance property of the exoskeleton manipulator. An admittance control approach is firstly presented based on the measurable force in order to generate a differentiable reference trajectory in interaction tasks. Then a stability criterion can be obtained due to the proposed control method. The designed controller includes linearly parameterization and estimation for the unknown items of the dynamics. Bounded and convergent error is shown in the tracking process while the robustness of the variable stiffness control method is guaranteed. The control approach is then verified on a robotic exoskeleton interacting with human via experiments. The results show that the presented approach can make for an effective pHRI performance.

Index Terms—Admittance control, Variable stiffness, Human-Robot Interaction, Robotic exoskeleton.

I. INTRODUCTION

Physical Human-Robot Interaction (pHRI) has become a feasible project since humanoid robots get developed in a great extent, as well as the development of control theories and researches about sensors that concerned in tactile sensing in this field. As the progress in application of robots goes, the interaction has been focused much more in physical ways, both in industry and service use. Such kind of applications in collaborative performance with robots have obtained satisfactory effects in both industrial and family domains. A kind of exoskeleton robot is developed, especially used in medical rehabilitation, and witnesses that such interaction systems between humans and robots can be more efficient. In order to better deal with the coordinating performance between human and robot, this paper propose a method on handling the interaction force and make the robotic limbs executed according to the human movements.

Admittance control accepts a force as input and reacts outputs as the robot motions. The appropriate choice of the mass, damper and spring coefficients can make the admittance control conform to the required effect. Hogan initiated the concept and method about impedance control [1], [2], which rapidly became a widely used control form for cooperative external force. Such method can solve the instability issues generated by force control performed on the end effector of the manipulator. But if impedance control is to be performed, the model of the robots and the interaction dynamics are required [3], [4]. As the dual form of the above approach, admittance

control has also been widely used in the applications of pHRI. In [5], admittance control with virtual force is presented to make the robot perform accurately in dancing state, which is an extreme application in pHRI. In [6], the motions and movement of robots are generated by the external human force. The admittance control scheme makes a framework that contain an outer-loop and an inner-loop, where the robot is able to track the output of the admittance model caused by the outer-loop. However, the control method does not contain a specific performance task model or a human dynamic model. In [7], an omni-directional type cane robot is described in a transfer function but the virtual spring and damper coefficient are both constant and the authors neglected the stiff coefficient in the admittance controller. In [8], admittance control is presented in pHRI. The robotic model is described as a spring-mass-damper system with the three coefficient being constants.

Recently, pHRI is implemented in the controlling of exoskeletons and robots with tactile sensing devices to achieve compliance between humans and robots by different forms of admittance control [9]. In [9], safety in admittance control is emphasized in the process of pHRI and small impedance is shown in the control method while the required acceleration is limited. However, the method can make compliant tasks, with no trajectory tracking purpose.

The adaptation or learning process is being studied when humans learn to contact a robotic equipment, where the process includes two parts. The first one contains the learning process of a robotic model to make the compensation for the robot dynamics. In [10], the optimal parameters of the impedance are obtained from a natural algorithm in robot interaction tasks. In [11], an interaction between robots and unknown steady environments is performed by a proposed adaptive impedance learning. The second part contains the learning process of a control loop which validates the effect of the cooperative tasks that relate to a human-robot model. In [12], variable impedance control is performed in the task of minimizing an objective function, using an algorithm of reinforcement learning which a path integral in it. The tasks of pHRI are dealt in this way using adaptive impedance control approaches. These researches show that controllers for such specific tasks should be closed in the outer-loop which contains human factors as well as a desired model for the performance.

Additionally, reference learning should also be taken into consideration in order to acquire the ideal learning performance, besides the impedance learning process mentioned above [13]. In the researches of the autonomously controlled robots, track planning has been widely studied without physi-

cal interaction with external environment [14], [15]. In [16], an approach of adaptive control is presented in order to track the desired trajectory of the robotic joints. Although the effect of the tracking performance is guaranteed as the control purpose, the interaction force is seen as an item of external disturbance and the compliance between the external force and robot is not taken into consideration. The field of pHRI has also involved the using of reference learning, where the movement of human is obtained for the update of the robot's trajectory and then the interaction would be compliant according to the motions of human's and the robot's. In [17], reference learning is used in the collaborative tasks between humans and robots where human characteristics of motions are taken into consideration. The intended movement of human is estimated by the robot and is used to control the manipulator while admittance control is to yield compliance with the interaction force. In [18], a method is proposed to reshape the reference trajectory but it is only to get controlled for a robotic system where the impedance model is given while constraint conditions are satisfied meanwhile.

In the typical case of a cooperative task considering both human and robot, impedance control is used to make compliance to the human's interaction force. So the robot is able to keep steps with the movement of human in this way. However, if the human trends to change his intention of movement, the interaction force will be treated as a load from outside so the previous trajectory will not be reference any more. To get a solution to this issue, researches on the adaptation of the robot's trajectory will be taken studied in order to obtain the regulation with the force being zero, and robot's reference trajectory will be updated in this process. Consequently, the energy of the human in interaction tends to be reduced so that the task of pHRI can realize the ideal efficiency.

Based on above discussions, a control framework is proposed in this paper to accomplish the adaptive admittance control scheme with time-varying stiffness parameter. The proposed approach can deal with human's motion intention so that it can perform more accurately in the actually physical interaction. This control approach is able to apply to humans of different skill levels and variant force powers without prior offline model tuning, and the robustness is guaranteed when changing the dynamics of robots. The control scheme consists of an inner loop and an outer loop. The former is to linearize the dynamics of the robot in a feedback way, while the latter is to tune the interaction model considering the intention of humans. The interaction model is shown in Fig. 1 and the overall control framework is shown in Fig. 2. The contributions of this paper are as follows:

- (1) The reference trajectory of the robotic exoskeleton would be reshaped according to the human-robot interaction force and the set desired trajectory.
- (2) The stiffness coefficient in the impedance model can be obtained through the stiffness observer.
- (3) An adaptive controller is developed in order to approximate the uncertain nonlinear robotic dynamics.

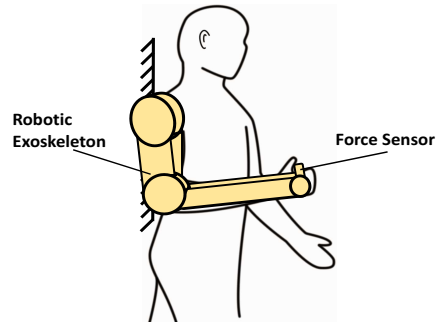


Fig. 1. Human-robot interaction task model

II. PRELIMINARIES AND PROBLEM FORMULATION

The dynamics of an n -link robotic exoskeleton interacting with an external force (the interaction model is shown in Fig. 1) can be described as follow:

$$M(q)\ddot{q} + C(q, \dot{q})\dot{q} + G(q) + f_{dis}(t) = \tau + \tau_e(t) \quad (1)$$

where $q \in \mathbb{R}^n$ is the position coordinates of the robotic joints, $\tau \in \mathbb{R}^n$ is the applied torque as the input item and $\tau_e \in \mathbb{R}^n$ is the torque in interaction tasks with the environment (or human), $M(q) \in \mathbb{R}^{n \times n}$ is an inertia matrix of symmetric positive definite, while $G(q) \in \mathbb{R}^n$ is the force of gravity, and $C(q, \dot{q}) \in \mathbb{R}^{n \times n}$ is considered as the centripetal and Coriolis torques, $f_{dis}(t) \in \mathbb{R}^n$ is considered as the external disturbance to the robot system. The terms $M(q)$, $C(q, \dot{q})$, and $G(q)$ include uncertain dynamic parameters.

The following properties are shown:

Property 1: [23] The matrix $\dot{M}(q) - 2C(q, \dot{q})$ is skew-symmetric.

Property 2: [24] Its inverse $M^{-1}(q)$ exists, and is also positive definite and bounded, i.e. $\|M^{-1}(q)\| < \alpha_{M^{-1}}$, where $\alpha_{M^{-1}}$ is a positive constant.

Property 3: [25] The exoskeleton dynamics (1) is linear in a set of physical parameters $W = [w_1, \dots, w_m]^T \in \mathbb{R}^m$ for any differentiable vector $\zeta \in \mathbb{R}^n$, then we have

$$M(q)\dot{\zeta} + C(q, \dot{q})\zeta + G(q) = Y(q, \dot{q}, \zeta, \dot{\zeta})W \quad (2)$$

where $Y(q, \dot{q}, \zeta, \dot{\zeta}) \in \mathbb{R}^{n \times m}$ is called the dynamic regressor matrix.

We transform the joint space into task space and the relation yields

$$x = \Omega(q), \quad \dot{x} = J(q)\dot{q} \quad (3)$$

According to (1), we let $x_1 = [q_1, q_2, q_3, \dots, q_n]^T$, $x_2 = [\dot{q}_1, \dot{q}_2, \dot{q}_3, \dots, \dot{q}_n]^T$, and $F_x = J^{-T}\tau_e$, where x_1 is the actual trajectory, x_2 is the actual velocity and F_x is the interaction force. The purpose of the control is to make the joint variable x_1 keep tracking the reference path x_r while there exists an interaction force. In addition, the closed loop signals are required to be bounded and converged as well as preventing the position constraints $|x_{1,i}(t)| < k_{c_i}$, $i = 1, 2, \dots, n$, from being violated $\forall t > 0$.

The following assumptions are proposed in order to make an easier design for the proof of the theorems.

Assumption 1: Positive constants $k_{d_i}, i = 1, 2, \dots, n$ are exist, such that $|x_{r_i}(t)| \leq k_{d_i} < k_{c_i}, i = 1, \dots, n, \forall t \geq 0$.

Assumption 2: A positive constant $F_{x_{m}}$ exists, so we have $\|F_x(t)\| \leq F_{x_{m}}, \forall t \geq 0$, where $F_{x_{m}}$ denotes the maximum of the interaction force.

III. ADAPTIVE ADMITTANCE CONTROL DESIGN

The generation of compliant motion is involved in the approach of admittance control. Admittance control accepts a force as input and produces robot motion as output. In this section, the first part is to shape a reference trajectory for the tracking task, which can represent the human subject's intention motions, so that the manipulator can get its behavior when the interaction force exists. The second part is the design of the motion control in order to get tracking of the reference trajectory shaped in the first part. The reference trajectory is generated in a constrained range, and then adaptive control scheme is proposed based on a backstepping approach for tracking.

A. Reference Trajectory Shaping

The method of shaping the reference trajectory is presented in this part. While interacting with human, the manipulator will track a new trajectory that deviates from the desired trajectory, which is due to human's intention. We assume that the process of adapting to the desired trajectory is to minimize the following cost function:

$$\Phi = \int_0^T \|F_x\|_R + \|x(\delta) - x_d(\delta)\|_G d\delta \quad (4)$$

where $\|\cdot\|_R$ and $\|\cdot\|_G$ are norms of the matrix while R and G are weights. Then there is a balance between human force and the error of the reshaped trajectory.

An impedance model for the exoskeleton is used to solve the cost function (4):

$$M(\ddot{x} - \ddot{x}_d) + D(\dot{x} - \dot{x}_d) + K(x - x_d) = F_x \quad (5)$$

where x is the position of the exoskeleton joint, x_d is its desired position, M is the inertia matrix, D is the damping matrix and K is the stiffness matrix, F_x is the interaction force. The external force for interaction and the error in the tasks can also be regulated using the above model, and x_d is the initial desired trajectory. x and F_x solved form (5) will minimize Φ in the cost function.

The above equation can be equivalently written as :

$$w = (\ddot{x} - \ddot{x}_d) + K_D(\dot{x} - \dot{x}_d) + K_P(x - x_d) - K_F F_x \quad (6)$$

where w, x, x_d and their first and second derivatives are functions of the time t and $K_D = M^{-1}D, K_P = M^{-1}k, K_F = M^{-1}$.

In order to reshape the reference trajectory, the parameters in the impedance model are needed to obtain first. The work in [19] has proposed a real-time method for measuring the variable stiffness parameter.

Let $\ddot{y} = \ddot{x} - \ddot{x}_d, \dot{y} = \dot{x} - \dot{x}_d$ and $y = x - x_d$. We consider a mass-damper-spring system $f = \ddot{y} + K_D\dot{y} + K_P y$, where f is the applied force. Now we consider a force function $h(y, u)$, taking the place of the spring item and we can obtain:

$$f = \ddot{y} + K_D\dot{y} + h(y, u) \quad (7)$$

The stiffness to be obtained is:

$$\frac{\partial f}{\partial y} = \frac{\partial h(y, u)}{\partial y} = \sigma(y, u) \quad (8)$$

Take the differential form of (7) with respect to time:

$$\dot{f} = \ddot{y} + K_D\dot{y} + \sigma\dot{y} + h_u\dot{u} \quad (9)$$

where $h_u = \frac{\partial h(y, u)}{\partial u}$. The estimate of \dot{g} is shown:

$$\dot{\hat{f}} = \ddot{y} + K_D\dot{y} + \hat{\sigma}\dot{y} \quad (10)$$

where $\hat{\sigma}$ is the estimate of stiffness and the update law is given:

$$\dot{\hat{\sigma}} = \alpha \hat{f} \text{sgn}(\dot{y}) \quad (11)$$

with $\dot{\hat{f}} = \dot{\hat{f}} - \dot{f}, \alpha > 0$ and:

$$\text{sgn}(t) = \begin{cases} \frac{t}{\|t\|}, & \|t\| \neq 0 \\ 0, & \|t\| = 0 \end{cases} \quad (12)$$

It is shown in [19] that the estimate stiffness $\hat{\sigma}$ is convergent to the actual stiffness with an uniformly ultimately bounded error.

In this paper, we employ an adaptive approach to obtain the human's intention reference trajectory [20]:

$$x_r(t + \Delta t) = x_r(t) - Lz(t) \quad (13)$$

where t denotes the current time in the adaption process and Δt denotes the constant time interval during the adaption. At the initial time t_0 , the trajectory is initialized as the desired trajectory, i.e. $x_r(t_0) = x_d(t_0)$. L is a constant matrix that would make the reference trajectory convergent and the item $z(t)$ is defined as follow:

$$z = (\dot{x} - \dot{x}_d) + \Lambda(x - x_d) - f_e \quad (14)$$

Where z, \dot{x} and \dot{x}_d are functions of the time t , z is the combination of the position error and velocity error with Λ being the weight of the two items while performing tracking, and f_e is the filtered force, defined below (18). Then we have:

$$\dot{z} = (\ddot{x} - \ddot{x}_d) + \dot{\Lambda}(x - x_d) + \Lambda(\dot{x} - \dot{x}_d) - \dot{f}_e \quad (15)$$

such that

$$w = \dot{z} + \Gamma z = (\ddot{x} - \ddot{x}_d) + (\Lambda + \Gamma)(\dot{x} - \dot{x}_d) + (\dot{\Lambda} + \Gamma\Lambda)(x - x_d) - (\dot{f}_e + \Gamma f_e) \quad (16)$$

Compared to (6), we have coefficients as the following form:

$$K_D = \Gamma + \Lambda, \quad K_P = \dot{\Lambda} + \Gamma\Lambda \quad (17)$$

$$\dot{f}_e + \Gamma f_e = K_F F_x \quad (18)$$

The coefficient K_P is got by the stiffness observer updated by (11), and the coefficient K_D is obtained by the relation between the stiffness and the damper, $K_D = \sqrt{2} * \overline{K_P}$. The

inertia coefficient is set to be an identity matrix in this paper. In summary, we have the following theorem for the adaption of the reference trajectory.

Theorem 1: Considering the human-robot interaction dynamics (1) that satisfies Assumption (1) and Assumption (2), using the impedance model (5) and the trajectory adaptation algorithm (13) under the control proposed later in (27), the objective (6) can be minimized to 0.

The proof can be found in Appendix A.

In the next section, we will propose an adaptive control with regressors to approximate the unknown dynamics parameters and to track the reference trajectory.

B. Control Design

In this part, we assume that full state information q and \dot{q} are available. According to (1), if we let $x_1 = [q_1, q_2, q_3, \dots, q_n]^T$, $x_2 = [\dot{q}_1, \dot{q}_2, \dot{q}_3, \dots, \dot{q}_n]^T$, then the dynamics of the interaction task can be shown in the following form:

$$\dot{x}_1 = x_2 \quad (19)$$

$$\dot{x}_2 = M^{-1}[\tau + \tau_e - f_{dis} - G - Cx_2] \quad (20)$$

Now that discrete points of the reference trajectory are got according to (13), a continuous trajectory is needed to be fitted online. Here Bezier curve is employed. The definition of a parametric Bezier curve can be expressed as follow:

$$Q(u) = \sum_{i=0}^p A_i J_{p,i}(u), \quad 0 \leq u \leq 1 \quad (21)$$

where u is a normalized parameter, p is the degree of the curve and A_i is the i th control point of the Bezier curve. The i th Bezier function $J_{p,i}(u) = {}^p C_i u^i (1-u)^{p-i}$, and $u^i (1-u)^{p-i}$ is the blending function, ${}^p C_i = \frac{p!}{(p-i)!i!}$. Here a three degree Bezier curve defined by 4 control points is used to achieve the continuous trajectory:

$$\begin{aligned} x_p(u) &= \sum_{i=0}^3 A_i J_{p,i}(u) \\ &= A_0(1-u)^3 + 3A_1u(1-u)^2 \\ &\quad + 3A_2u^2(1-u) + A_3u^3 \\ &= a_0 + a_1u + a_2u^2 + a_3u^3 \end{aligned} \quad (22)$$

where A_0, A_1, A_2, A_3 are control points and a_0, a_1, a_2, a_3 are the corresponding coefficients. According to [21], the radius of curvature varies smoothly in this Bezier curve for its high order differential is existing. So that we can get the continuous reference trajectory $x_r^* = x_p(u)$. The error z_1 and z_2 are defined as follow:

$$z_1 = x_1 - x_r^* \quad (23)$$

$$z_2 = x_2 - \alpha_1 \quad (24)$$

where the item α_1 is the virtual control to z_1 and its definition can be found in Appendix B. Considering an n-DOF robotic manipulator, $\alpha_1 \in \mathbb{R}^n$, $z_1 \in \mathbb{R}^n$ and $z_2 \in \mathbb{R}^n$.

$$\dot{z}_1 = \dot{x}_1 - \dot{x}_r^* = z_2 + \alpha_1 - \dot{x}_r \quad (25)$$

Once if the parameters of the dynamics are all known, a control method is expressed in the following form:

$$\tau = -z_1 - K_2 z_2 + f_{dis} + G + C\alpha_1 + M\dot{\alpha}_1 - \tau_e \quad (26)$$

Nevertheless, there is no easy ways to get the precise information of disturbance f_{dis} as well as the terms of the robotic dynamics including G, C, M . To get a solution, Property 3 is applied in order to make an approximation of the unknown dynamics. Moreover, the external disturbance is estimated by an observer. Such that:

$$\tau = -z_1 - K_2 z_2 + Y(Z)\hat{W} + \hat{f} - \tau_e \quad (27)$$

with $K_2 \in \mathbb{R}^{n \times n}$ and $\lambda_{\min}(K_2) > 0$, and \hat{f} is the high-order disturbance observer, and the disturbance observer is given as the following form:

$$\begin{cases} \dot{\hat{f}} &= \hat{z} + K_d x_2 \\ \dot{\hat{z}} &= -K_d \hat{z} + K_d (Y_d(Z_d)\hat{W}_d - K_d x_2) \end{cases} \quad (28)$$

where $Y_d(Z_d) \in \mathbb{R}^{n \times m}$ is the dynamic regressor matrix, the definition of Z and Z_d are given in Appendix B, and $K_d^T = K_d > 0$. $W \in \mathbb{R}^m$ and $W_d \in \mathbb{R}^m$ are physical parameters and their updating laws are designed as:

$$\dot{\hat{W}}_i = -\Gamma_i (Y_i(Z) z_{2i} + \theta_i \hat{W}_i) \quad (i = 1, 2, \dots, n) \quad (29)$$

$$\dot{\hat{W}}_{di} = -\Gamma_{di} (Y_{di}(Z) \hat{f}_i + \theta_{di} \hat{W}_{di}) \quad (i = 1, 2, \dots, n) \quad (30)$$

where θ_i and θ_{di} are small positive real numbers, $\Gamma_i > 0$, and $\Gamma_{di} > 0$. The linear characteristic of the regressor is also used for estimating the parameters in the disturbance observer.

$$Y(Z)W^* = G(x_1) + C(x_1, x_2)\alpha_1 + M\dot{\alpha}_1 - \epsilon \quad (31)$$

$$Y_d(Z_d)W_d^* = \tau + \tau_e - C(x_1, x_2)x_2 - G(x_1) - \epsilon_d \quad (32)$$

where W^* and W_d^* are optimal estimations and ϵ and ϵ_d are estimate errors of the dynamics. ϵ and ϵ_d satisfy $\max_{Z \in \Omega_Z} |\epsilon| < \epsilon^*$ and $\max_{Z_d \in \Omega_{Z_d}} |\epsilon_d| < \epsilon_d^*$ respectively [24].

Theorem 2: Consider the the robotic dynamics (19) and (20), using (27), together with (28), and the adaptive laws (29) and (30), and the overall control scheme is shown in Fig. 2, the control signals of the closed-loop system, z_1, z_2, \tilde{W} , and \tilde{W}_d are semiglobally bounded. Furthermore, the error signals z_1, z_2, \tilde{W} , and \tilde{W}_d will be kept in the compact sets $\Omega_{z_1}, \Omega_{z_2}, \Omega_{\tilde{W}}$, and $\Omega_{\tilde{W}_d}$ respectively, defined as follow:

$$\Omega_{z_1} := \left\{ z_1 \in \mathbb{R}^n \mid \|z_{1i}\| \leq \sqrt{D_1} \right\} \quad (33)$$

$$\Omega_{z_2} := \left\{ z_2 \in \mathbb{R}^n \mid \|z_{2i}\| \leq \sqrt{\frac{D_1}{\lambda_{\min}(M)}} \right\} \quad (34)$$

$$\Omega_{\tilde{W}} := \left\{ \tilde{W} \in \mathbb{R}^n \mid \|\tilde{W}_i\| \leq \sqrt{\frac{D_1}{\lambda_{\min}(\Gamma^{-1})}} \right\} \quad (35)$$

$$\Omega_{\tilde{W}_d} := \left\{ \tilde{W}_d \in \mathbb{R}^n \mid \|\tilde{W}_{di}\| \leq \sqrt{\frac{D_1}{\lambda_{\min}(\Gamma_d^{-1})}} \right\} \quad (36)$$

where $D_1 = 2(V_2^*(0) + \frac{B_1}{\kappa_1})$ with κ_1 and B_1 given in (70) and (71), where both are positive definite.

The proof can be found in Appendix B and the overall

control framework is shown in Fig. 2.

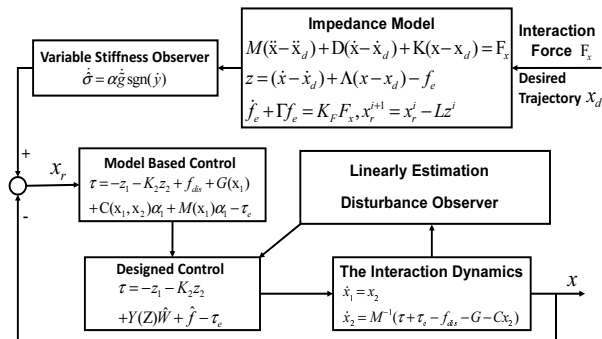


Fig. 2. Block diagram of the control scheme

IV. EXPERIMENTS

Experiments of the proposed adaptive control schemes are designed to verify the effectiveness in this section. Experiments are done on the robotic exoskeleton located in our key lab of Autonomous System and Network Control. Two DC motors are equipped for the experimental robot system as actuators and the selection of the actuators is on the basis of our actual needed torque in experiments and the external force in the tasks. The motor driver is chosen as Elmo SOL-WHI5/60E01 and the maximum baud rate of the CAN bus is 1Mbit/s. The loop frequency of the control loop is 25Hz and the maximum sampling rate of the sensors is 5MHz.

Fig. 3 presents the experimental platform, which contains the robotic system with a force sensor, a unit of the executive drivers and an industrial personal computer (IPC). The executive drivers are used to generate a driving torque for the actuators and gather the motion information in the tasks from the force sensor and encoders of actuators, while the IPC is used to execute the programs that involve the control on the experiment platform.

We examine the control performance for the control schemes proposed in this paper. The gains of the controller are given: $K_1 = \text{diag}[24.5, 30.6]$, $K_2 = \text{diag}[3.3, 2.1]$, $K_d = \text{diag}[1.2, 1.8]$. The gain matrix Γ_i and $\Gamma_{d,i}$ are defined as $\Gamma_1 = 0.01I$, $\Gamma_2 = 0.01I$, $\Gamma_{d,1} = 0.04I$, and $\Gamma_{d,2} = 0.04I$. Small positive constants θ_i and $\theta_{d,i}$ are chosen as $\theta_1 = 0.5$, $\theta_2 = 0.5$, $\theta_{d,1} = 0.1$ and $\theta_{d,2} = 0.1$.

Three experiment subjects participated in the experiment. Table 1 shows the relevant information of the three subjects. During the task of the experiment, the subject holds the end-effector and moves according to his own intention back and forth in an appropriate range, which can be expressed by the shaped reference trajectory. An interaction force is generated and is measured by the force sensor equipped at the end of the robotic exoskeleton. With the adaptive control method proposed in this paper, the interaction force will decrease and the errors of tracking the reference trajectory are convergent.

Table 1: Information of the experimenters

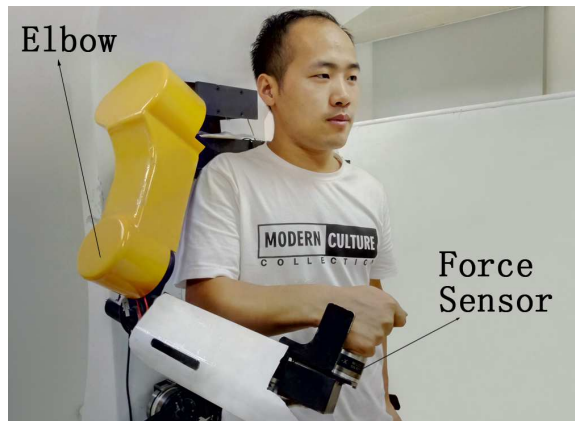


Fig. 3. The experimental interaction system model

Experimenter	Age	Weight	Force in the Experiment
Subject. 1	24	54.5 kg	Shown in Fig. 7
Subject. 2	23	56.5 kg	Shown in Fig. 11
Subject. 3	22	62.1 kg	Shown in Fig. 15

The results are shown in Figs. 4 - 15. Figs. 4, 8 and 12 show the tracking situation of the shoulder joint (q_1) and the elbow joint (q_2) of the 3 subjects. The tracking error demonstrated in Figs. 5, 9 and 13 shows convergence and bounded in the experiment tasks.

Figs. 6, 10 and 14 show the output of the stiffness observer proposed in Section III-A which is updated by (11). Values of the interaction force are collected by the force sensor at the end point of the elbow joint and is shown in Figs. 7, 11 and 15. Under the adaptive admittance control schemes proposed in this paper, the interaction force is gradually reduced synchronously with the adaption of the stiffness estimated by the observer. The reducing of the interaction force can demonstrate that the robotic exoskeleton is showing compliance to the human behaviour during the interaction task. In summary, from these results we can see that our proposed control approach is effective in the actual physical interaction between human and robot.

V. CONCLUSION

As is shown in this paper, the framework of the adaptive admittance control is proposed, which includes the estimate of the movement of human intention. The inner-loop is to linearize the dynamics of the robot in a feedback way, while the outer-loop is to tune the interaction model considering the intention of humans. The use of the regressor can linearize the unknown dynamics of the robot in the inner-loop such that the effect of the work performed in the outer-loop can be ensured. Three groups of experiments are displayed in the last section, with experimenters of different ages and levels of interaction forces. The results show the virtue of the proposed admittance control in dealing the tasks of physical interaction between humans and robots, and the control approach, without prior offline model tuning, can also be robust when the dynamics of robots change. Tests about even more interaction tasks will be done in our future work, as well as models

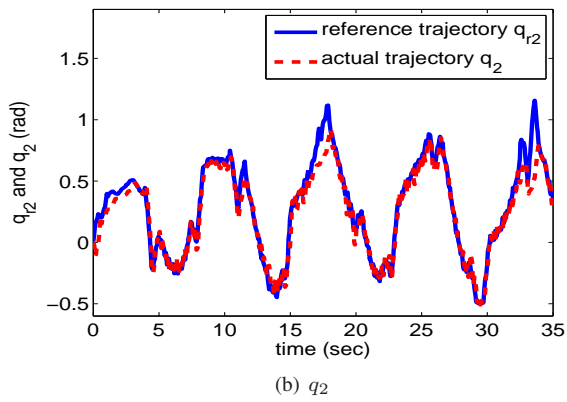
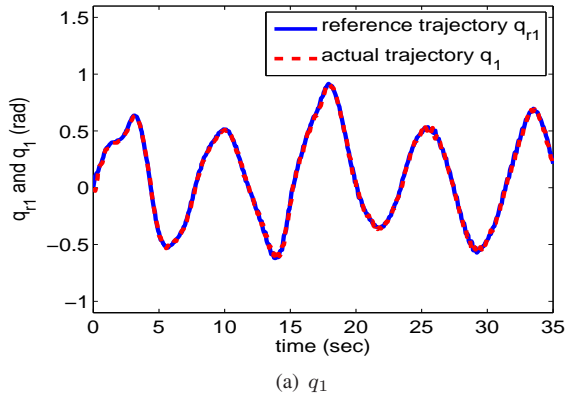


Fig. 4. The tracking performance of Subject. 1

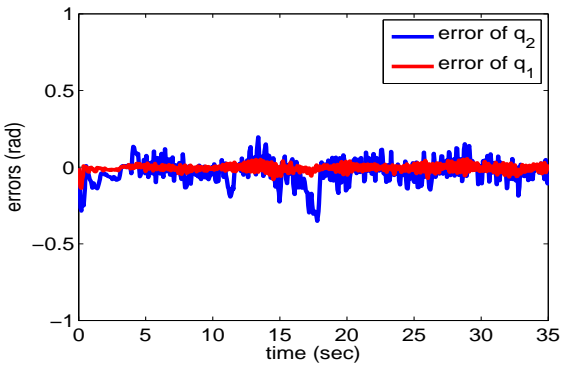


Fig. 5. The tracking error of Subject. 1

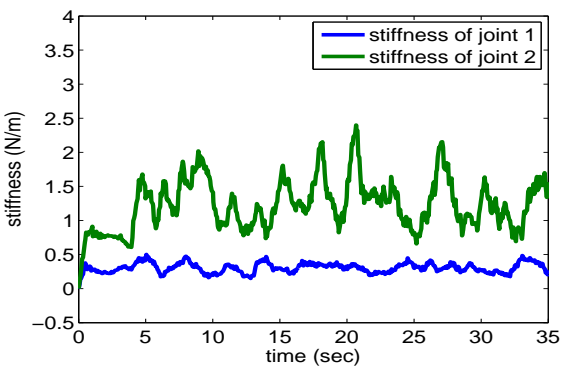


Fig. 6. The stiffness of Subject. 1

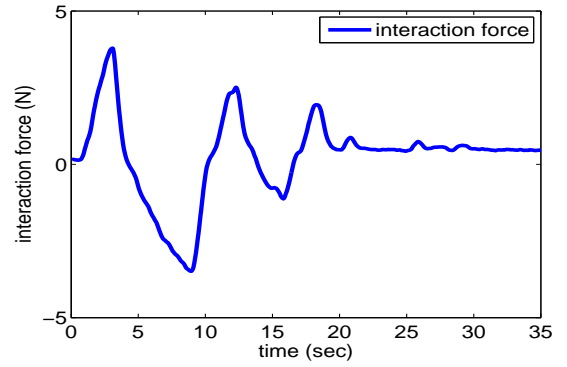


Fig. 7. The interaction force of Subject. 1

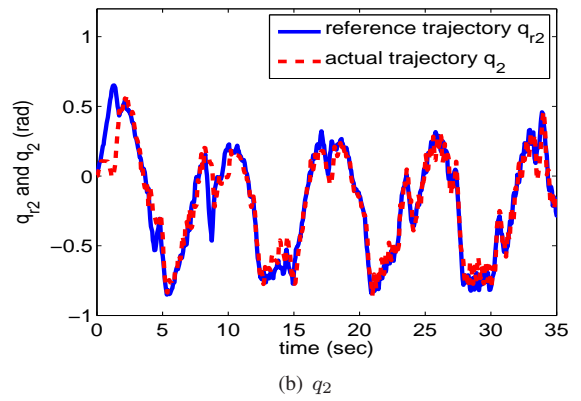
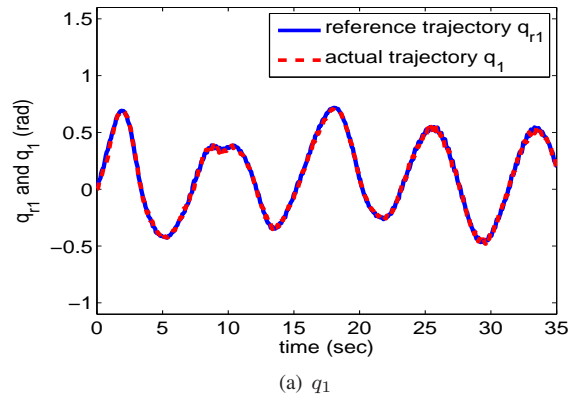


Fig. 8. The tracking performance of Subject. 2

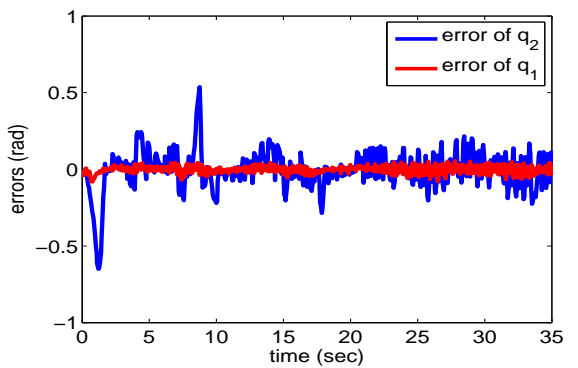


Fig. 9. The tracking error of Subject. 2

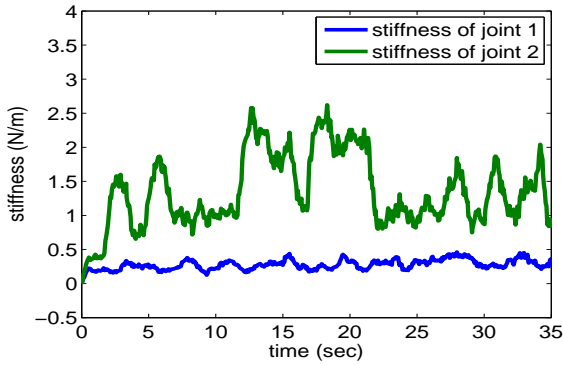


Fig. 10. The stiffness of Subject. 2

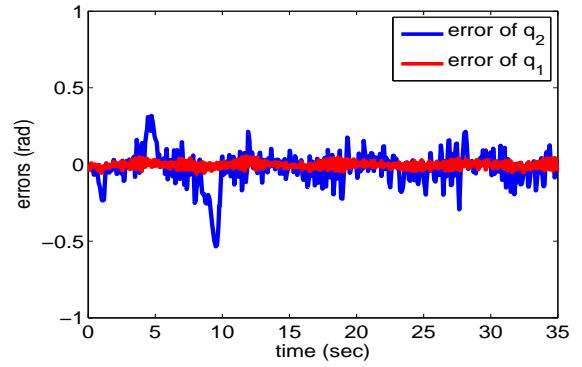


Fig. 13. The tracking error of Subject. 3

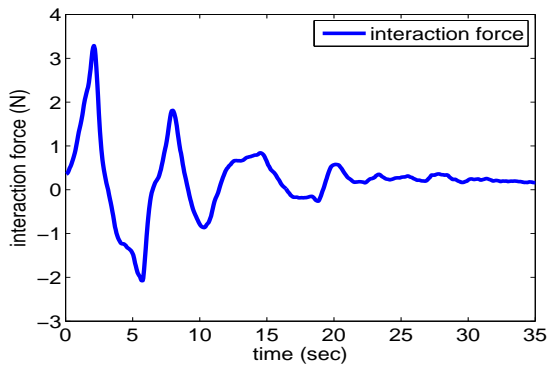


Fig. 11. The interaction force of Subject. 2

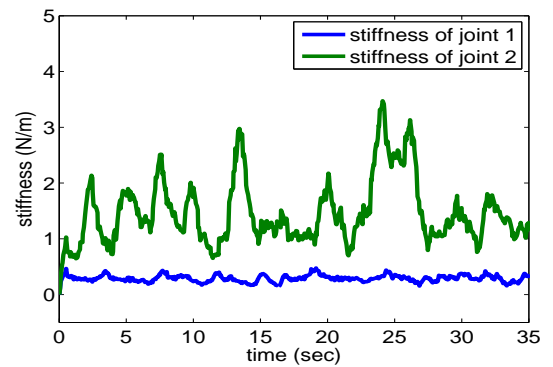


Fig. 14. The stiffness of Subject. 3

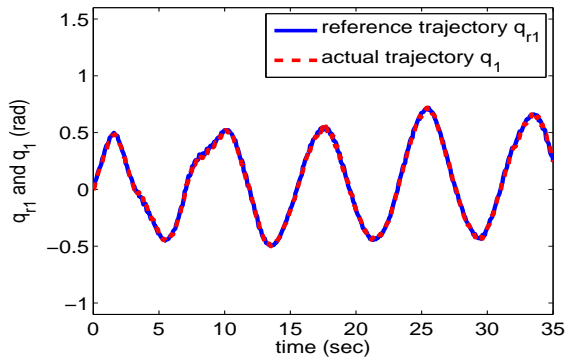
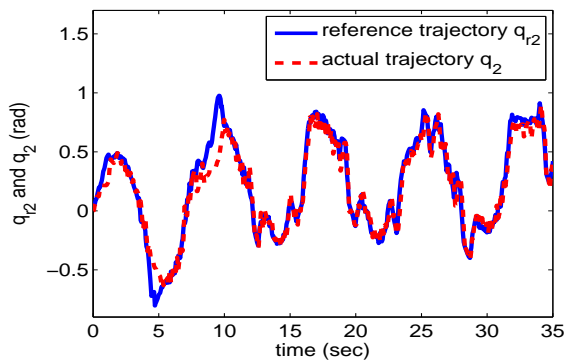
(a) q_1 (b) q_2

Fig. 12. The tracking performance of Subject. 3

with new forms of estimation of human intentions and more complex performances in task space.

APPENDIX A PROOF OF THEOREM 1

Lemma 1: [26] Considering that signals $g(t)$, $\alpha(t)$, and $h(t)$ satisfying the following condition:

$$g(t) \leq \alpha(t) + \int_0^t h(\delta)g(\delta)d\delta, \quad (37)$$

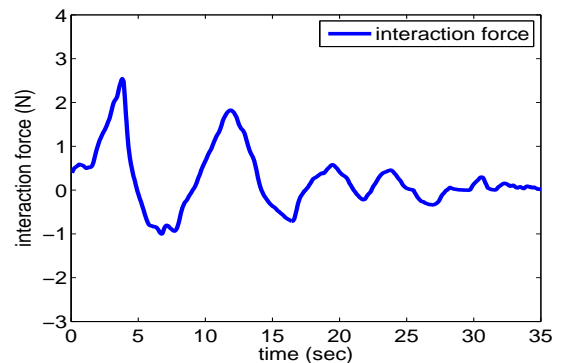


Fig. 15. The interaction force of Subject. 3

then we have:

$$g(t) \leq \alpha(t) + \int_0^t \alpha(\delta)h(\delta)e^{\int_\delta^t h(s)ds}d\delta. \quad (38)$$

Combining the control law (27), and z_1 (23), z_2 (24), we can change the control τ into the following form:

$$\tau = -K(x - x_r) - K_2(\dot{x} - \dot{x}_r) + Y(Z)\hat{W} + \hat{f} - \tau_e \quad (39)$$

where $K = K_2\Gamma$ is the stiffness coefficient and the control is function of time t . We define:

$$s_r(t) = Kx_r(t) + K_2\dot{x}_r(t) \quad (40)$$

$$s(t) = Kx(t) + K_2\dot{x}(t) \quad (41)$$

where $\dot{x}_r(t) = \frac{1}{\Delta t}(x_r(t) - x_r(t - \Delta t))$, then from (13) and (16), we have:

$$\begin{aligned} s_r(t + \Delta t) &= Kx_r(t + \Delta t) + K_2\dot{x}_r(t + \Delta t) \\ &= s_r(t) - K_2Lw(t) \end{aligned} \quad (42)$$

By defining $x = x_e$ as the equilibrium trajectory that satisfies the following equation:

$$(\ddot{x}_e - \ddot{x}_d) + K_D(\dot{x}_e - \dot{x}_d) + K_P(x_e - x_d) = K_FF_e \quad (43)$$

Then we have $w = 0$ and F_e is the external force when $x = x_e$. The actual trajectory is initialized at the initial time: $x(t_0) = x_d(t_0)$. Substituting control (39) into the interaction dynamics, we can get:

$$M(x)\ddot{x} + C\dot{x} + G + f_{dis} = -s + s_r + Y\hat{W} + \hat{f} \quad (44)$$

With the equilibrium trajectory x_e , we can also define the equilibrium reference trajectory x_{re} that satisfies:

$$M(x_e)\ddot{x}_e + C\dot{x}_e + G + f_{dis} = -s_e + s_{re} + Y\hat{W} + \hat{f} \quad (45)$$

where $s_e = Kx_e + K_2\dot{x}_e$ and $s_{re} = Kx_{re} + K_2\dot{x}_{re}$ deriving from (40), and $w = 0$ when $x = x_{re}$.

Considering that $N(x, \dot{x}) = C\dot{x} + G + f_{dis} - Y\hat{W} - \hat{f} + s$, so (44) and (45) can be written as follow:

$$M(x)\ddot{x} + N(x, \dot{x}) = s_r \quad (46)$$

$$M(x_e)\ddot{x}_e + N(x_e, \dot{x}_e) = s_{re} \quad (47)$$

Defining $\Delta M = M(x) - M(x_e)$, $\Delta N = N(x, \dot{x}) - N(x_e, \dot{x}_e)$, $\Delta x = x - x_e$, $\Delta s_r = s_r - s_{re}$, $\Delta F = F_x - F_e$. Combining (46), (47), (43) and (16), we have:

$$\Delta\ddot{x} = M^{-1}(x)(\Delta s_r - \Delta N - \Delta M\ddot{x}_e) \quad (48)$$

$$w = \Delta\ddot{x} + K_D\Delta\dot{x} + K_P\Delta x - K_F\Delta F \quad (49)$$

where $\Delta\ddot{x}$ and w are functions about the time t . From (43), (49), and the definition that $\Delta s_r(t + \Delta t) = s_r(t + \Delta t) - s_r(t)$, $\Delta s_r(t) = s_r(t) - s_r(t - \Delta t)$, we have:

$$\begin{aligned} \Delta s_r(t + \Delta t) &= -K_2L(\Delta\ddot{x} + K_D\Delta\dot{x} \\ &\quad + K_P\Delta x - K_F\Delta F) \end{aligned} \quad (50)$$

We consider n_L , n_{M1} , n_K , n_D , n_P , n_F , n_2 as the $\|\cdot\|_\infty$ norm of L , M^{-1} , K_2 , K_D , K_P , K_F , \ddot{x}_e respectively in the compact set of finite time. The function $N(x, \dot{x})$ is continuously derivable so it satisfies the Lipschitz condition

[27]. We have Lipschitz coefficients l_n , l_m , l_f of $N(x, \dot{x})$, $M(x)$ and F_x . From (48) and (50), take norm of both sides and there is a constant u_0 that yields

$$\|\Delta\ddot{x}\| \leq n_{M1}\|\Delta s_r\| + u_0\|\Delta x, \Delta\dot{x}\| \quad (51)$$

$$\begin{aligned} \|\Delta s_r(t + \Delta t)\| &\leq \|K_2LM^{-1}\|\|\Delta s_r(t)\| \\ &\quad + \|K_2L\|\left(\|M^{-1}\|\|\Delta N\| \right. \\ &\quad \left. + \|M^{-1}\ddot{x}_e\|\|\Delta M\| + \|K_D\|\|\Delta\dot{x}\| \right. \\ &\quad \left. + \|K_P\|\|\Delta x\| + \|K_F\|\|\Delta F\|\right) \\ &\leq q\|\Delta s_r(t)\| + u_1\|\Delta x, \Delta\dot{x}\| \end{aligned} \quad (52)$$

Note that $q = \|K_2LM^{-1}\| < 1$ and $u_1 = n_Kn_L(n_{M1}l_n + n_{M1}n_2l_m + n_D + n_P + n_Fl_f)$. Using integral and the consideration of $\Delta x(0) = 0$, then we have:

$$\begin{aligned} \|\Delta x(t), \Delta\dot{x}(t)\| &\leq \int_0^t \left((u_0 + 1)\|\Delta x(\delta), \Delta\dot{x}(\delta)\| \right. \\ &\quad \left. + n_{M1}\|\Delta s_r(\delta)\| \right) d\delta \end{aligned} \quad (53)$$

From Lemma 1, multiply both sides by $e^{-\alpha t}$, such that

$$e^{-\alpha t}\|\Delta x, \Delta\dot{x}\| \leq n_{M1} \int_0^t e^{-\alpha\delta}\|\Delta s_r\|e^{(u_0+1-\alpha)(t-\delta)}d\delta \quad (54)$$

As is shown in [28], $\forall M(t), \|M(t)\|_\alpha = \sup(e^{-\alpha t}\|M(t)\|)$, then the following inequation holds that $\|M(t)\|_\alpha \leq \|M(t)\|_\infty \leq e^{\alpha t}\|M(t)\|_\alpha$. So the above inequation (54) can be changed as:

$$\begin{aligned} \|\Delta x, \Delta\dot{x}\|_\alpha &\leq n_{M1}\|\Delta s_r\|_\alpha \int_0^t e^{(u_0+1-\alpha)(t-\delta)}d\delta \\ &\leq q_1\|\Delta s_r\|_\alpha \end{aligned} \quad (55)$$

Note that $q_1 = \left\| \frac{n_{M1}(1-e^{(u_0+1-\alpha)T})}{\alpha-u_0-1} \right\|$, where T is the finite time interval. Combining (51), we have:

$$\|\Delta\ddot{x}\|_\alpha \leq q_2\|\Delta s_r\|_\alpha \quad (56)$$

where $q_2 = n_{M1} + u_0q_1$. From (49), we have:

$$\begin{aligned} \|w\|_\alpha &\leq \|\Delta\ddot{x}\|_\alpha + u_2\|\Delta x, \Delta\dot{x}\|_\alpha \\ &\leq q_3\|\Delta s_r\|_\alpha \end{aligned} \quad (57)$$

where $u_2 = n_D + n_P + n_Fl_F$, $q_3 = q_2 + u_2q_1$. Combining (52) and (55), we have:

$$\begin{aligned} \|\Delta s_r(t + \Delta t)\|_\alpha &\leq q\|\Delta s_r(t)\|_\alpha + u_1q_1\|\Delta s_r(t)\|_\alpha \\ &\leq q_4\|\Delta s_r(t)\|_\alpha \end{aligned} \quad (58)$$

where $q_4 = q + \frac{u_1n_{M1}(1-e^{(u_0+1-\alpha)T})}{\alpha-u_0-1}$. Here if we make α large enough, then we get $q_4 < 1$, $\|\Delta s_r\|_\alpha \rightarrow 0$, such that $\|\Delta s_r\| \rightarrow 0$. Then from (57), $w \rightarrow 0$ is guaranteed.

APPENDIX B PROOF OF THEOREM 2

Lemma 2: [22] If a Lyapunov function $V(x)$ exists in the consideration of initially bounded, which is positive definite and C^1 continuous, and satisfies $\kappa_1(\|x\|) \leq V(x) \leq \kappa_2(\|x\|)$, such that $\dot{V}(x) \leq -\kappa V(x) + c$, where κ_1, κ_2

: $\mathbb{R}^n \rightarrow \mathbb{R}$ are class \mathcal{K} functions, while both κ and c are positive constants, then the solution to the Lyapunov function, $x(t)$, is uniformly bounded.

Consider Lyapunov function candidate $V_1 = \frac{1}{2}z_1^T z_1$. Time derivative of V_1 is

$$\dot{V}_1 = z_1^T \dot{z}_1 = z_1^T (z_2 + \alpha_1 - \dot{x}_r^*) \quad (59)$$

If we let $\alpha_1 = \dot{x}_r^* - K_1 z_1$ with $K_1 \in \mathbb{R}^{n \times n}$ and $\lambda_{\min}(K_1) > 0$, the above Lyapunov function can be changed in the following form:

$$\dot{V}_1 = -z_1^T K_1 z_1 + z_1^T z_2 \quad (60)$$

then, we can get:

$$\begin{aligned} \dot{z}_2 &= \dot{x}_2 - \dot{\alpha}_1 \\ &= M^{-1}[\tau + \tau_e(t) - f_{dis} - G - Cx_2] - \dot{\alpha}_1 \end{aligned} \quad (61)$$

where $\dot{\alpha}_1 = -K_1 \dot{z}_1 + \ddot{x}_r^*$. We consider a Lyapunov function $V_2 = V_1 + \frac{1}{2}z_2^T M z_2$, so the time derivative form of V_2 will be

$$\begin{aligned} \dot{V}_2 &= \dot{V}_1 + z_2^T M \dot{z}_2 + \frac{1}{2}z_2^T \dot{M} z_2 \\ &= -z_1^T K_1 z_1 + z_1^T z_2 + z_2^T (\tau + \tau_e - f_{dis} \\ &\quad - G - Cx_2 - M\dot{\alpha}_1 + \frac{1}{2}\dot{M} z_2) \end{aligned} \quad (62)$$

Applying Property 1, we have

$$\dot{V}_2 = -z_1^T K_1 z_1 + z_1^T z_2 + z_2^T (\tau + \tau_e - f_{dis} - G - C\alpha_1 - M\dot{\alpha}_1) \quad (63)$$

Substituting control (27) into (63)

$$\begin{aligned} \dot{V}_2 &= -z_1^T K_1 z_1 - z_2^T K_2 z_2 - z_2^T \epsilon \\ &\quad - z_2^T f_{dis} + z_2^T \hat{f} + z_2^T Y(Z) \tilde{W} \end{aligned} \quad (64)$$

where $Z = [x_1^T, x_2^T, \alpha_1^T, \dot{\alpha}_1^T]$ and $Z_d = [\tau^T, x_1^T, x_2^T]$. Given $\tilde{W} = \hat{W} - W^*$ and $\tilde{W}_d = \hat{W}_d - W_d^*$. By considering the effect of \tilde{W} to the stability of the control system, the following Lyapunov candidate is suggested

$$\begin{aligned} V_2^* &= V_2 + \frac{1}{2} \sum_{i=1}^n \tilde{W}_i^T \Gamma_i^{-1} \tilde{W}_i + \frac{1}{2} \hat{f}^T \hat{f} \\ &\quad + \frac{1}{2} \sum_{k=1}^n \tilde{W}_{dk}^T \Gamma_{dk}^{-1} \tilde{W}_{dk} \end{aligned} \quad (65)$$

Derivative of V_2^* about time and substitute (64) into it

$$\begin{aligned} \dot{V}_2^* &= \sum_{i=1}^n (z_{2,i} Y_i(Z) \tilde{W}_i + \tilde{W}_i^T \Gamma_i^{-1} \dot{\tilde{W}}_i) \\ &\quad + \sum_{k=1}^n \tilde{W}_{dk}^T \Gamma_{dk}^{-1} \dot{\tilde{W}}_{dk} - z_1^T K_1 z_1 - z_2^T K_2 z_2 \\ &\quad - z_2^T \epsilon - z_2^T f_{dis} + \hat{f}^T \dot{\hat{f}} + z_2^T \dot{\hat{f}} \end{aligned} \quad (66)$$

Consider the disturbance observer (28), the disturbance observer error is defined as $e_f = \hat{f} - f_{dis}$, and we have

$$\dot{e}_f = \dot{\hat{f}} - \dot{f}_{dis} = -K_a e_f - \dot{f}_{dis} - K_d Y_d(Z_d) \tilde{W}_d \quad (67)$$

where $K_a = \min\{K_{id}, K_{id} \alpha_{M-1}\}$. With the disturbance observer error signals (67), and the updating laws (29) - (30), we have:

$$\begin{aligned} \dot{V}_2^* &= -z_1^T K_1 z_1 - z_2^T K_2 z_2 - z_2^T \epsilon + z_2^T \dot{\hat{f}} - z_2^T f_{dis} \\ &\quad - \sum_{i=1}^n \theta_i \tilde{W}_i^T \dot{\tilde{W}}_i - \sum_{k=1}^n \theta_{dk} \tilde{W}_{dk}^T \dot{\tilde{W}}_{dk} \\ &\quad - \hat{f}^T K_a e_f \end{aligned} \quad (68)$$

Since $-\tilde{W}_i^T \dot{\tilde{W}}_i = -\tilde{W}_i^T (W_i^* + \tilde{W}_i) = -\tilde{W}_i^T \tilde{W}_i - \tilde{W}_i^T W_i^*$ and $-\tilde{W}_i^T W_i^* \leq \frac{1}{2}(\tilde{W}_i^T \tilde{W}_i + W_i^{*T} W_i^*)$, we have $-\tilde{W}_i^T \dot{\tilde{W}}_i \leq -\frac{1}{2}\tilde{W}_i^T \tilde{W}_i + \frac{1}{2}W_i^{*T} W_i^*$. Similarly, $-\tilde{W}_{di}^T \dot{\tilde{W}}_{di} \leq -\frac{1}{2}\tilde{W}_{di}^T \tilde{W}_{di} + \frac{1}{2}W_{di}^{*T} W_{di}^*$. And $z_2^T \epsilon \leq z_2^T z_2 + \frac{1}{2}\epsilon^T \epsilon \leq z_2^T z_2 + \frac{1}{2}\|\epsilon^*\|^2$, $-z_2^T f_{dis} \leq \frac{1}{2}z_2^T z_2 + \frac{1}{2}\|f_M^*\|^2$. Substitute these inequalities and $e_f = \hat{f} - f_{dis}$ into (68)

$$\begin{aligned} \dot{V}_2^* &\leq -z_1^T K_1 z_1 - z_2^T (K_2 - 2I_{n \times n}) z_2 \\ &\quad - \sum_{i=1}^n \frac{1}{2} \theta_i \tilde{W}_i^T \tilde{W}_i - \sum_{k=1}^n \frac{1}{2} \theta_{dk} \tilde{W}_{dk}^T \tilde{W}_{dk} \\ &\quad + \frac{1}{2} \|\epsilon^*\|^2 + \frac{1}{2} \|f_M^*\|^2 + \sum_{i=1}^n \frac{1}{2} \theta_i W_i^{*T} W_i^* \\ &\quad + \sum_{k=1}^n \frac{1}{2} \theta_{dk} W_{dk}^{*T} W_{dk}^* \\ &\quad - \hat{f}^T (K_a - I) \hat{f} + \frac{1}{2} \|K_a\|^2 \|f_M^*\|^2 \\ &\leq -\kappa_1 V_2^* + B_1 \end{aligned} \quad (69)$$

where

$$\begin{aligned} \kappa_1 &= \min \left(2\lambda_{\min}(K_1), 2\lambda_{\min}(K_a - I), \right. \\ &\quad \left. \frac{2\lambda_{\min}(K_2 - 2I_{n \times n})}{\lambda_{\max}(M)}, \min_{i=1,2,\dots,n} \left\{ \frac{\theta_i}{\lambda_{\max}(\Gamma_i^{-1})} \right\}, \right. \\ &\quad \left. \min_{k=1,2,\dots,n} \left\{ \frac{\theta_{dk}}{\lambda_{\max}(\Gamma_{dk}^{-1})} \right\} \right) \end{aligned} \quad (70)$$

$$\begin{aligned} B_1 &= \frac{1}{2} \|\epsilon^*\|^2 + \sum_{i=1}^n \frac{1}{2} \theta_i W_i^{*T} W_i^* + \frac{1 + \|K_a\|^2}{2} \|f_M^*\|^2 \\ &\quad + \sum_{k=1}^n \frac{1}{2} \theta_{dk} W_{dk}^{*T} W_{dk}^* \end{aligned} \quad (71)$$

To ensure $\kappa_1 > 0$, the design parameters $\theta_i > 0$, $\theta_{dk} > 0$, $K_1 = K_1^T > 0$ and $K_2 - 2I_{n \times n} = (K_2 - 2I_{n \times n})^T > 0$ and $K_a - I_{n \times n} = (K_a - I_{n \times n})^T > 0$. Integrating (69) over $[0, t]$, we can get

$$\begin{aligned} \dot{V}_2^* &\leq (V_2^*(0) - \frac{B_1}{\kappa_1}) e^{-\kappa_1 t} + \frac{B_1}{\kappa_1} \\ &\leq V_2^*(0) + \frac{B_1}{\kappa_1} \end{aligned} \quad (72)$$

According to the Lemma 2, the system stability is guaranteed.

REFERENCES

- [1] N. Hogan, "Adaptive control of mechanical impedance by coactivation of antagonist muscles." *IEEE Transactions Automatic Control*, vol. 29, no.

- 8, pp. 681–690, 1984.
- [2] N. Hogan, “Impedance control an approach to manipulation. I- Theory. II- Implementation. III -Applications,” *Transaction of the ASME, Journal of Dynamic Systems, Measurement, and Control*, vol. 107, pp. 1-24, 1985.
- [3] S. K. Singh and D. O. Popa, “An analysis of some fundamental problems in adaptive control of force and impedance behavior: theory and experiments,” *IEEE Transactions on Robotics and Automation*, vol. 11, no. 6, pp. 912-921, Dec. 1995.
- [4] H. Kazerooni, T. Sheridan, and P. Houpt, “Robust compliant motion for manipulators, part I: The fundamental concepts of compliant motion,” *IEEE Journal of Robotics and Automation*, vol. 2, no. 2, pp. 83-92, June 1986.
- [5] H. Wang, K. Kosuge, “Control of a Robot Dancer for Enhancing Haptic Human-Robot Interaction in Waltz,” *IEEE Transaction on Haptics*, VOL. 5, NO. 3, pp. 264–273, 2012.
- [6] I. Ranatunga, F. L. Lewis, D. O. Popa, and S. M. Tousif, “ Adaptive admittance control for humanCrobot interaction using model reference design and adaptive inverse filtering,” *IEEE Transactions on Control System Technology*, In Press.
- [7] K. Wakita, J. Huang, P. Di, K. Sekiyama, T. Fukuda, “Human-walking-intention-based motion control of an omnidirectional-type cane robot,” *IEEE/ASME Transaction on Mechatronics*, vol. 18, no. 1, pp. 285–296, 2013.
- [8] V. Okunev, T. Nierhoff, S. Hirche, “Human-preference-based Control Design: Adaptive Robot Admittance Control for Physical Human-Robot Interaction,” in *2012 IEEE RO-MAN: The 21st IEEE International Symposium on Robot and Human Interactive Communication*, pp. 443–448, 2012.
- [9] A. Morbi and M. Ahmadi, “Safely rendering small impedances in admittance-controlled haptic devices,” *IEEE/ASME Transactions on Mechatronics*, vol. 21, no. 3, pp. 1272-1280, Jun. 2016.
- [10] B. Kim, J. Park, S. Park, and S. Kang, “Impedance learning for robotic contact tasks using natural actor-critic algorithm,” *IEEE Transactions on Systems, Man, and Cybernetics*, vol. 40, no. 2, pp. 433-443, Apr. 2010.
- [11] S. S. Ge, Y. Li, and C. Wang, “Impedance adaptation for optimal robotC environment interaction,” *International Journal of Control*, vol. 87, no. 2, pp. 249-263, 2014.
- [12] J. Buchli, F. Stulp, E. Theodorou, and S. Schaal, “Learning variable impedance control,” *International Journal of Robotics Research*, vol. 30, no. 7, pp. 820-833, 2011.
- [13] P. Dizio and J. R. Lackner, “Motor adaptation to coriolis force perturbations of reaching movements: Endpoint but not trajectory adaptation transfers to the nonexposed arm,” *Journal of Neurophysiology*, vol. 74, no. 4, pp. 1787-1792, 1995.
- [14] J. Barraquand and J.-C. Latombe, “Robot motion planning: A distributed representation approach,” *International Journal of Robotics Research*, vol. 10, no. 6, pp. 628-649, 1991.
- [15] A. Saccon, J. Hauser, and A. Beghi, “Trajectory exploration of a rigid motorcycle model,” *IEEE Transactions on Control Systems Technology*, vol. 20, no. 2, pp. 424-437, Mar. 2012.
- [16] S. Ito, M. Darainy, M. Sasaki, and D. J. Ostry, “Computational model of motor learning and perceptual change,” *Biological Cybernetics*, vol. 107, no. 6, pp. 653-667, 2013.
- [17] B. Corteville, E. Aertbelien, H. Bruyninckx, J. De Schutter, and H. V. Brussel, “Human-inspired robot assistant for fast point-to-point movements,” in *Proc. International Conference on Robotics and Automation*, Rome, Italy, 2007, pp. 3639-3644.
- [18] K. P. Tee, R. Yan, and H. Li, “Adaptive admittance control of a robot manipulator under task space constraint,” in *Proceedings of IEEE International Conference on Robotics and Automation*, Anchorage, AK, USA, 2010, pp. 5181-5186.
- [19] G. Grioli and A. Bicchi, “A Non-invasive Real-Time Method for Measuring Variable Stiffness,” *Proceedings of Robotics: Science and Systems*, Zaragoza, Spain, 2010.
- [20] C. Yang and E. Burdet, “A Model of Reference Trajectory Adaptation for Interaction with Objects of Arbitrary Shape and Impedance,” in *2011 IEEE/RSJ International Conference on Intelligent Robots and Systems*, San Francisco, CA, USA, 2011, pp. 4121–4126.
- [21] K. G. Jolly, R. S. Kumara, R. Vijayakumar, “A Bezier curve based path planning in a multi-agent robot soccer system without violating the acceleration limits,” in *Robotics and Autonomous Systems*, pp. 23–33, 2009.
- [22] S. S. Ge and C. Wang, “Adaptive neural network control of uncertain MIMO non-linear systems,” *IEEE Transactions on Neural Networks*, vol. 15, no. 3, pp. 674–692, 2004.
- [23] Z. Li, C. Yang, and L. Fan, *Advanced Control of Wheeled Inverted Pendulum Systems*. London, U.K.: Springer-Verlag, 2012.
- [24] S. S. Ge, C. C. Hang, T. H. Lee, and T. Zhang, *Stable Adaptive Neural Network Control*. Boston, USA: Kluwer Academic, 2001.
- [25] M. W. Spong, S. Hutchinson, and M. Vidyasagar, *Robot Modeling and Control*. New York: Wiley, 2006.
- [26] G. Tao, “Adaptive Control Design and Analysis,” Hoboken, NJ: John Wiley and Sons, 2003.
- [27] M. Hirsch and S. Smale, “Differential Equations, Dynamical Systems, and Linear Algebra,” San Diego, CA: Academic Press, Inc, 1974.
- [28] D. Wang and C. C. Cheah, “An iterative learning-control scheme for impedance control of robotic manipulators,” *The International Journal of Robotics Research*, vol. 17, no. 10, pp. 1091-1099, 1998.